Penerbit Akademia Baru

CFD Letters

Journal homepage: www.akademiabaru.com/cfdl.html
ISSN: 2180-1363

Design and Analysis of Vortex Induced Vibration (VIV) Suppression Device

Open Access

Syamsul Azry Md Esa[1], Wan Mohd. Arif Aziz Japar[2], Nor Azwadi Che Sidik[2,*]

[1] Faculty of Mechanical Engineering, Universiti Teknologi Malaysia, 81310 Utm Johor Bahru, Malaysia
[2] Malaysian-Japan International Institute of Technology (MJIIT), Universiti Teknologi Malaysia, 54100 UTM Kuala Lumpur, Malaysia

ARTICLE INFO

Article history:
Received 3 October 2018
Received in revised form 15 January 2019
Accepted 24 January 2019
Available online 10 February 2019

Keywords:
Riser, Vortex induced vibration, Suppression device, Structural enhancement, Fairing

ABSTRACT

Riser which have a cylindrical structure is used in Oil & Gas industry to facilitate the safe transportation of material, fluids, and gases between seafloor and host platform. However, the continues interaction between the cylinder riser and shed vortices causes a several damage to the riser due to large amplitude of vibration experienced by the riser. As consequence, maintenance cost and time consuming to repair the damage increases. Hence, present study is conducted to investigate the effectiveness of fairing geometry to suppress vortex induced vibration of a cylindrical structure. Comparative analysis between bare cylinder and the proposed design is conducted to study the effect of fairing geometry on the drag coefficient and lift coefficient of proposed design. The result shows the existence of fairing geometry in proposed design has obtained the lower St number then cylinder riser and thus reduced the vortex shedding formation near to main structure. Besides that, vortex shedding formed by the proposed design is less aggressive and slower than bare cylinder. At the lower velocity (v = 0.5m/s), proposed design with the chord length of 1.5D shows the lowest CL and CD value. However, at the higher velocity (1.0m/s≤v≤2.0m/s), proposed design with the chord length of 1.25D shows the lowest CL value with average drag coefficient.

1. Introduction

Marine Riser is a conductor pipe which connected between an offshore platform that floating in an ocean such as storage platform or vessel with seabed (Figure 1(a)) [1]. The marine riser can be classified into two functions, production riser and drilling riser. The main function of production riser is to facilitate the safe transportation of material, fluids, and gases between seabed and storage platform while drilling riser is used to provides a pathway for drilling and transport drilling mud [2]. As shown in Figure 1(b), the riser system always exposed to the heavy load from currents and waves of ocean. As a result, the riser will experience the large deflection and if it happens continuously, it will damage the riser due to fatigue in riser system. Intensive studies have been conducted by former

* *Corresponding author.*
E-mail address: azwadi@utm.my (Nor Azwadi Che Sidik)

research on dynamic analysis and vibration control in order to ensure the safety and to enhance the durability and productivity of riser.

(a) (b)

Fig. 1. Oil & Gas offshore (a) Host platform (b) Cylinder riser

The riser or conductor can be either rigid or flexible connection between a platform and a wellhead on seabed. Figure 2 illustrates the typical location and configuration of the riser or conductor.

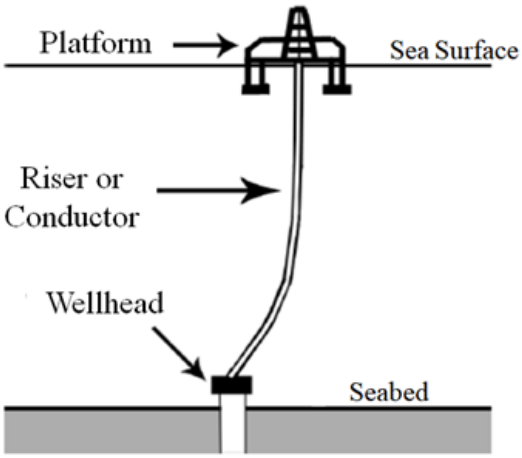

Fig. 2. Regimes of Fluid Flow across Smooth Circular Cylinders

As mention before, VIV of structures is one of the practical interest to many fields of engineering. Cylindrical structures such as marine risers in deepwater applications are prone to this phenomenon, which is due to the regular shedding of vortices from the riser when exposed to unsteady current flow. The main purposes of this structure is not to gain lift or minimize drag as it is with aircraft components, but rather to bear loads, contain flow, or provide heat transfer surfaces [3]. Association of VIV in the interaction between fluids and riser is subjected to extensive researches in both industries and academic field over the past few decades due to high demand in exploring hydrocarbon resources.

Karman vortex shedding occurs due to the flow separation around any structure [4]. When the vortex shedding frequencies are synchronized with natural frequencies of a riser along a considerable length, the system is said to be in a “lock in” range. As a result, the conductor pipe will experience extensive oscillations or vibrations, which can lead to high frequency cyclic stresses, resulting in

unacceptable high rates of fatigue damage or premature failure to the structure [5]. Siti Hajar *et al.,* [6] also has studied about how the flow frequency affects the vortex shedding frequency. This detrimental effect is severe for drilling risers, and even more so for production risers where service life in excess of 25 years are often required. Generally, deepwater risers are most susceptible to complex VIV response because current flow intensity can be different along the different depths in deepwater areas. There are two possible motions of a cylinder structure such as riser when subject to current flow, namely the in-line motion and transverse or cross-flow motion. Figure 3 shows the direction of the possible motions for a cylinder when subjected to a current flow.

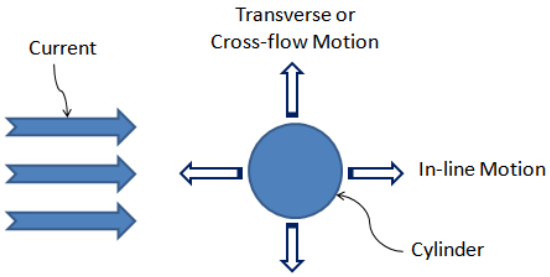

Fig. 3. Regimes of Fluid Flow across Smooth Circular Cylinders

Studies on the vibration of circular cylinders in oscillating flow began with structures exposed to open ocean waves in marine engineering applications. Morison *et al.,* [7] proposed a modelling method where the force on the structure in oscillating flow is expressed as the summation of inertia and drag forces. A lot of researchers still used this method. There are a number of CFD-based VIV studies.

Generally, unwanted vibration can be controlled by two strategies such as passive method [8-12] and active method [13-15]. In passive method, the strategies including structural damping, modification of the riser's structural rigidity, internal fluid's velocity, the top tension and vortex-suppression device. Vortex-suppression device is the most applicable strategy in passive method. In 2018, Azlin *et al.,* [16] studied the effect circular cylinder with and without shroud geometry on vortex formation. They revealed that, the formation length was greater at gap ratio of 2.0 than that at 1.6, with smaller wake width observed in a former in comparison to that in a latter.

latter While in active method, the vibration control strategy is adjusting the external flow rate such as proportional-integral control and boundary control [17].

Rahman *et al.,* [18] studied the unsteady flow passed a circular cylinder using a 2D finite volume method with different Reynolds number. They found that, as Reynolds number becomes higher than 40, the flow shows a loss of symmetry in the wake. The studied also reported the Strouhal number (St) is found to be 0.164 for Re=100. Vijaya *et al.,* [19] investigated 2D unsteady flows of power-law fluids over a cylinder. The study has been solved using a finite volume method as solver. The result shows that, in unsteady flow, lift coefficient and Strouhal number increase as Re number increases.

Mittal and Kumar [20] studied VIV on a pair of equal-size cylindrical cylinders with two sets of arrangement, inline and staggered. The fixed cylinders for the 2D simulation were simulated in a rectangular computational domain with a fixed Reynold number of Re = 1000. They concluded that for a circular cylinder, flow separation point changes with Reynolds number, so the wake is unsteadiness. They also concluded that the oscillations of the cylinders result in an alternate mode of vortex shedding and where the vibration of cylinders is usually accompanied by an increase in drag.

Shao and Zhang [21] used the finite volume method to investigate two side-by-side cylindrical cylinders. The cylinders were simulated in a 23 times of the cylinder diameter computational domain

with a constant inlet velocity of 7m/s. They concluded that LES is capable of reproducing complex subcritical turbulent wake behind a circular cylinder, but fine meshes and longer time were required for the flow around the circular cylinder. Bourguet *et al.,* [22] studied lock-in of the VIV on an in-line flow of a flexible cylindrical cylinder using direct numerical simulation (DNS) of the 3D incompressible Navier-Stokes equations. They concluded that the structural vibrations are mixtures of standing and traveling wave patterns. A frequency ratio of approximately 2 can be established between the excited frequencies in the in-line and cross-flow directions.

Pratish and Tiwari [23] investigate unsteady wakes behind two inline arrangement of square cylinders. 2D computational domain was used where the length and width of the channel were 16 times and 6 times of the square width cylinders. The result shows that, at the larger aspect ratio of cylinder, vortex shedding behind the downstream cylinder varnishes. Besides that, when the aspect ratio increases, the value of drag coefficient at upstream and downstream become more positive and negative, respectively. Chandrakant and Swapnil [24] analysed vortex shedding behind a D shaped cylinder. 2D computational domain with 2 m length and 1.6 m, and quad meshing was used for the study. They reported that the Strouhal number increases with increase in Reynolds number and the number of vortices increases with Reynolds number.

Ali and Edris [25] analysed the numerical simulation of unsteady flow with vortex shedding around circular cylinder. Two-dimensional flow of an incompressible fluid around a circular cylinder were simulated in both uniform stream flow and oscillated flows at Re = 300. The computational domain with length, 0.3 m and width, 0.2 m with water as the assumption liquid was used in the study. It can be observed, when the inlet flow frequency is increased, Strouhal number slightly increases and drag coefficient considerably increase.

Roshko [26] has conducted an experiment to investigate the formation of vortex shedding at high Reynold number. He found that vortex shedding was not observed at $Re < 3.5x10^6$. At the Re number lower than $3.5x10^6$, no peak frequency occurred, but above this value, strong spectral peak appeared. In 1996, John *et al.,* [27] pointed that the literature resources in fluid mechanics is not entirely comprehensible in defining the values for vortex frequency measurements for rigid circular cylinders. By tradition, several data sets have been accepted, although improved data are established from time to time. There are a lot of challenges faced by many previous researchers during 1960s, especially when many sets of data conflict with each other, and the variability of data results is overlooked.

Blevins [3] lists four recommendations in order to reduce VIV resonant substantially such as increase reduced damping, avoid resonance, streamline cross section and add vortex suppression device. The details explanation as shown below:

a) Increase Reduced Damping

The amplitude of vibration will be decreased if the reduced damping is increased. Particularly, the peak amplitudes at resonance are ordinarily less than 1% of the structure diameter, if the reduced damping exceeds the values of 64. During this period, the amplitudes can be considered negligible when compared to the deflection induced by drag. There are two main approaches to achieve the increment of reduced damping, by either increasing structural damping or increasing structural mass. Ordinarily, increased damping can be gained by permitting scraping or banging between structural elements, by using material with high internal damping such as viscoelastic material, rubber, and wood, or by using external dampers.

b) Avoid Resonance

Resonance is highly dependent on natural frequency of a structure. The natural frequency can be tuned, so that it will not overlapped with the frequency of a system driven by the external forces. This can be typically achieved by stiffening the structure, and this approach is most suitable for small structure due to weight and cost effect.

c) Streamline Cross Section

Vortex shedding can be minimized as well as drag can be reduced, if separation from the structure can be minimized. Streamlining is the most efficient and practical when the flow direction is fixed in relative to the structure and the structure has adequate stiffness to avoid flutter.

d) Vortex Suppression Device

There have number of device that can be used to supress VIV such as helical strake, perforated shroud, axial slats, streamlined fairing, splitter, ribbon or hair cable, guiding vane, spoiler plates and stepped cylinder. They work by disrupting or preventing the formation of an organized, two-dimensional vortex street.

All studies reviewed here shows flow characteristic around circular cylinder changes with flow behaviour of sea that act on the cylinder surface. Most of the studies have analysed the effect cylinder arrangement [20, 21, 23] on the VIV suppression performance. However, to the best of authors' knowledge, there has no study which analyse the use of Streamlined Fairing of passive method in VIV suppression for riser control in spite of the fact that it has the most lower drag coefficient than other passive VIV suppression devices at Re = 10^5 [3]. It also proven in comprehensive review that has been conducted by Hong K. S. *et al.,* [28] for the lack of data on Streamlined Fairing method. In the present study, comparative analysis has been conducted between cylinder riser and fairing riser in order to analyse the effect of fairing geometry on VIV formation. Besides that, the effect of fairing chord length has been analysed in order to find optimum geometry with lower drag coefficient and lift coefficient. Maximum fluid flow speed range used in this analysis according to the data obtained from met ocean for Malaysia region.

2. Methodology

2.1. Design Input

Cylinder with diameter of 0.5m is used in present study as it lies in one of the common range for riser and conductor in Oil & Gas industry. This size is neither too small nor too big for the application. Properties of water such as density and viscosity (kinematic and dynamic) are used instead of sea water because a lot of experimental data in laboratory use water. Cylinder is subjected to a flow speed of 0.5 m/s to 2.0 m/s with the incremental value of 0.5 m/s. These values are selected based on the typical maximum current fluid flow speeds of metocean data in Malaysia region for up to 100 years where in the extreme storm condition. When performing back calculation with the other inputs data, the flow speed that will be used in present analysis is in the range of Reynolds number between 10^5 and 10^6.

There are three configurations of riser cylinder being used in this study, namely bare cylinder, cylinder with chord length of 1.25D, and cylinder with chord length of 1.5D. Lower value of chord length is not considered due to the space required when installing the bearing mechanism to allow the fairing to be weathervane in actual condition. On the other hand, higher value of chord length is not included due to practicality of fairing in the application, whereby longer fairing chord length

contributes to greater weight as well as cost increases. The summary of design inputs is shown in Table 1.

Table 1
Design inputs

Item	Detail	Values
Geometry	Size of bare cylinder	0.5m
Fluid Properties (Water)	Density	998.2kg/m^3
	Dynamic Viscosity	1 x 10^{-3}kg/m-s
	Kinematic Viscosity	1 x $10^{-6}$$m^2$/s
Flow Speed	Four variations	0.5m/s
		1.0m/s
		1.5m/s
		2.0m/s
Corresponding Reynolds Number	Four variations	2.49X10^5
		4.98 X10^5
		7.46 X10^5
		9.95 X10^5
Fairing Chord Length	Two variations	1.25D
		1.5D

2.2. Design Variable

Speed of fluid flow or the Reynolds number (Re), and the cylinder configurations are the independent variables in this study. Three different configurations of cylinder are shown in Figure 4. The dependent variable or the parameter that are being extracted from the output of the analysis are drag coefficient (CD), lift coefficient (CL) and Strouhal number (St). Controlled variable or parameters that are being constant throughout the simulation are fluid temperature, fluid density and fluid viscosity (kinematic and dynamic). The summary of design variables is shown in Table 2.

Table 2
Details of variables

Independent Variables	Flow speeds / Reynolds number
	Fairing Chord Length
Dependent Variables	Drag coefficient, C_d
	Lift coefficient, C_L
	Strouhal Number
Controlled Variable	Fluid Temperature
	Fluid Density
	Fluid Viscosity

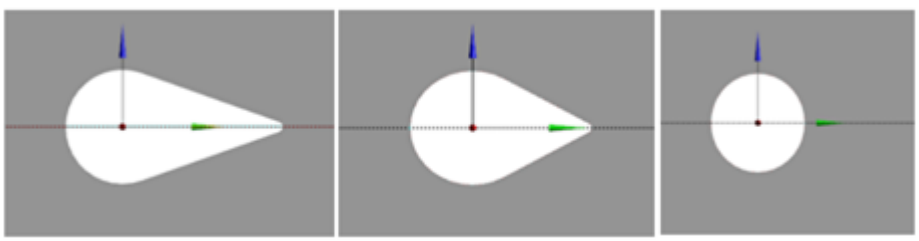

(a) (b) (c)

Fig. 4. Configurations of cylinder (a) Fairing 1.5D (b) Fairing 1.25D (c) Bare Cylinder

2.3. System Domain

Performing CFD analysis requires high usage of computational resources. Therefore, only 2-dimensional representation of simulation (surface body) is chosen to conduct the analysis numerically. The system domain consists of an inlet (left), an outlet (right), a 2-d cylinder (middle) and two walls (top and bottom).

The fluid flows from inlet to outlet through subject study (cylinder) with walls as boundary conditions. Sufficient area of system domain is created to compromise between output results and computational time. The cylinder has distance of 6D to the inlet, 15D to the outlet and 6D to both of side walls. The system domain is illustrated in Figure 5.

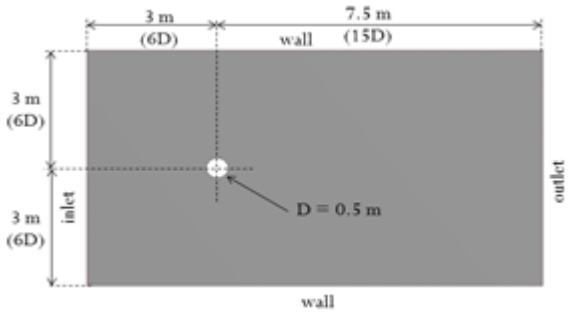

Fig. 5. System domain for analysis

2.4. Numerical Method Approach.

2.4.1. Governing equation

The CFD problems are stated in a set of mathematical equations and are solved numerically. These set of mathematical equations are based on the conservation laws of fluid motion, which are conservation of mass, conservation of momentum, conservation of energy and etc. For CFD problems related to fluid flow, the set of mathematical equations are based on the conservation of mass and momentum.

Eq. (1) is the general form of the mass conservation equation and it is valid for incompressible as well as compressible flows. The source is the mass added the system and any user-defined sources. The density of the fluid is ρ and the flow of mass in x, y and z directions are u, v and w, respectively.

$$\frac{\partial \rho}{\partial t}+\frac{\partial(\rho u)}{\partial x}+\frac{\partial(\rho v)}{\partial y}+\frac{\partial(\rho w)}{\partial z}=S_m \tag{1}$$

The conservation of momentum is originally expressed in Newton's second law. Momentum is a vector quantity as well as a magnitude. Momentum is also a conserved quality, meaning that for a closed system, the total momentum will not change as long as there is no external force. Newton's second law also states that the rate of momentum change of a fluid particle equals the sum of the forces on the particle. We can differentiate the rate of momentum change for x, y and z direction.

The mass conservation theory states that the mass will remain constant over time in a closed system. This means that the quantity of mass will not change and, the quantity is conserved. The mass conservation equation, also called the continuity equation can be written as:

$$\rho\frac{Du}{Dt};\rho\frac{Dv}{Dt};\rho\frac{Dw}{Dt} \tag{2}$$

The momentum conservation equation for x, y and z direction can be written as follows:

$$\rho\frac{Du}{Dt}=\frac{\partial\left(-p+\tau_{xx}\right)}{\partial x}+\frac{\partial\tau_{yx}}{\partial y}+\frac{\partial\tau_{zx}}{\partial z}+S_{mx} \tag{3}$$

$$\rho\frac{Dv}{Dt}=\frac{\partial\left(-p+\tau_{yy}\right)}{\partial y}+\frac{\partial\tau_{xy}}{\partial x}+\frac{\partial\tau_{zy}}{\partial z}+S_{my} \tag{4}$$

$$\rho\frac{Dw}{Dt}=\frac{\partial\left(-p+\tau_{zz}\right)}{\partial z}+\frac{\partial\tau_{xz}}{\partial x}+\frac{\partial\tau_{yz}}{\partial y}+S_{mz} \tag{5}$$

The source Sm is defined as contribution to the body forces in the total force per unit volume on the fluid. The pressure is a normal stress, is denoted p, whilst the viscous stresses are denoted by τ.

2.4.2. General Transport Equation

To derive the transport equation of viscous and incompressible fluids, the Navier-Stokes equation is used [29]. For a Newtonian fluid, which stress versus strain rate curve is linear, the Navier-Stokes equation for x, y and z direction is defined as follows:

$$\rho\frac{Du}{Dt}=-\frac{\partial p}{\partial x}+\frac{\partial}{\partial x}\left[2\mu\frac{\partial u}{\partial x}+\lambda divu\right]+\frac{\partial}{\partial y}\left[\mu\left(\frac{\partial u}{\partial y}+\frac{\partial v}{\partial x}\right)\right]+\frac{\partial}{\partial z}\left[\mu\left(\frac{\partial u}{\partial z}+\frac{\partial w}{\partial x}\right)\right]+S_{Mx} \tag{6}$$

$$\rho\frac{Dv}{Dt}=-\frac{\partial p}{\partial y}+\frac{\partial}{\partial y}\left[2\mu\frac{\partial v}{\partial y}+\lambda divu\right]+\frac{\partial}{\partial x}\left[\mu\left(\frac{\partial u}{\partial y}+\frac{\partial v}{\partial x}\right)\right]+\frac{\partial}{\partial z}\left[\mu\left(\frac{\partial v}{\partial z}+\frac{\partial w}{\partial y}\right)\right]+S_{My} \tag{7}$$

$$\rho\frac{Dw}{Dt}=-\frac{\partial p}{\partial z}+\frac{\partial}{\partial z}\left[2\mu\frac{\partial w}{\partial z}+\lambda divu\right]+\frac{\partial}{\partial x}\left[\mu\left(\frac{\partial u}{\partial z}+\frac{\partial w}{\partial x}\right)\right]+\frac{\partial}{\partial y}\left[\mu\left(\frac{\partial v}{\partial z}+\frac{\partial w}{\partial y}\right)\right]+S_{Mz} \tag{8}$$

Lambda (λ) is the dynamic viscosity, which relates stresses to linear deformation and μ is the second viscosity which relates stresses to the volumetric deformation. The value of a property per unit mass is expressed with φ.

Eq. (9) which is the transport equation consists of various transport processes. First term on left is the rate of change term or usually called the unsteady term, second term on left is the convective term, first term on right is the diffusion term and second term on right is source term.

$$\frac{\partial(\rho\phi)}{dt}+div(\rho\phi u)=div(\Gamma grad\phi)+S_{\phi} \tag{9}$$

2.4.3. Drag force and Lift force equation

As the result of the periodic change of the vortex shedding, the pressure distribution of the cylinder due to the flow will also change periodically, thereby generating a periodic variation in the force components on the cylinder. The force components can be divided into cross-flow and in-line directions. The force of the cross-flow direction is commonly named as the lift force (FL) while the latter is named as the drag force (FD).

The lift force appears when the vortex shedding starts to occur and it fluctuates at the vortex shedding frequency. Similarly, the drag force also has the oscillating part due to the vortex shedding, but in addition it also has a force as a result of friction and pressure difference; this part is called the mean drag. Both of the lift and drag forces are formulated as follows:

$$F_L = \hat{F}_L \sin(\omega_s t + \phi_s) \tag{10}$$

$$F_D = \overline{F}_D + \hat{F}_D \sin(2\omega_S t + \phi_S) \tag{11}$$

$\hat{F}_D$ and $\hat{F}_L$ are the amplitudes of the oscillating lift and drag respectively and $\overline{F_D}$ is a mean drag. The vortex shedding frequency is represented by $\omega_s = \frac{2\pi}{f_v}$, and ϕ_s is the phase angles between the oscillating forces and the vortex shedding. $\hat{C}_D$ and $\hat{C}_L$ are the dimensionless parameters for drag and lift forces respectively, and can be derived as:

$$\hat{C}_L = \frac{\hat{F}_L}{\frac{1}{2}\rho LDU^2} \tag{12}$$

$$\hat{C}_D = \frac{\hat{F}_D}{\frac{1}{2}\rho LDU^2} \tag{13}$$

$$\overline{C}_D = \frac{\overline{F}_D}{\frac{1}{2}\rho LDU^2} \tag{14}$$

where ρ, L, D and U are the fluid density, cylinder length, cylinder diameter and flow velocity respectively.

2.4.4. Mesh generation

At the initial stage, the size of elements is set to a coarse mesh structure, so that any solution glitch due to geometry creation could be detected with low time cost. If there has no abnormality found, meshing with finer mesh structure configurations is set up. The number of nodes and elements for the fine mesh structure that adopted in the present study are 54,085 and 75,796

respectively. The mesh structure in this paper is consist of quad and triad shape. Quad elements are concentrated at the critical area which is at the cylinder wall, while triad elements are located at the remaining locations. The mesh structure is developed by global mesh and local mesh. The local mesh is created by edge sizing and inflation method. This method is adopted in present study to ensure the mesh structure can produce accurate simulation result. The details of the mesh configuration are shown in Table 3 and the mesh structure is shown in Figure 6.

Table 3
Mesh Details

Item	Description	Detail
Statistical Data	Number of nodes	54,085
	Number of elements	75,796
Mesh Elements	Quad	At critical area (cylinder wall)
	Triad	Remaining location
Mesh Treatment	Inflation	First layer near to cylinder wall
	Edge Sizing	On cylinder wall

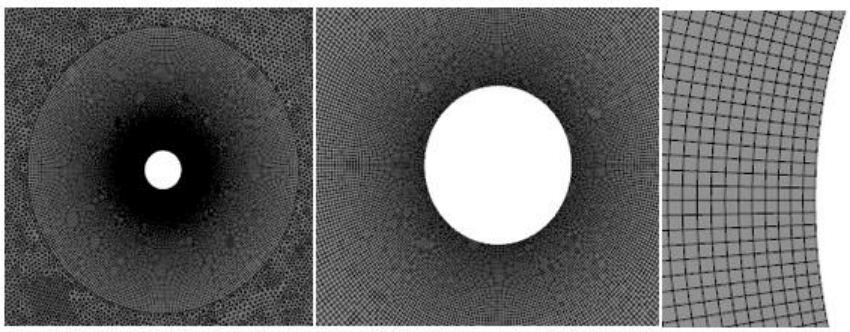

Fig. 6. Generated mesh in system domain

3. Results and Discussion

3.1. Validation of Numerical Model

The baseline model that being used throughout the different cylinder configurations, are determined based on the preliminary simulations performed in the Ansys Fluent software. After fine-tuning some miscellaneous parameters available in the software, two parameters such as the drag coefficient (CD), as well as Strouhal number (St) are used for validation purpose the results are shown in the following subsections.

The first validation for the baseline model is done using the comparison of the drag coefficient (CD) between the results obtained from preliminary simulations and the established plot of drag coefficient (CD) versus Reynolds number for a smooth cylinder. The second validation for the baseline model is done using the comparison of the Strouhal number (St) between the results obtained from preliminary simulations and the established plot of Strouhal number (St) versus Reynolds number for a smooth cylinder. Figure 7 shows the validation results for drag coefficient and Strouhal number when a bare cylinder is subjected to a flow with different speeds.

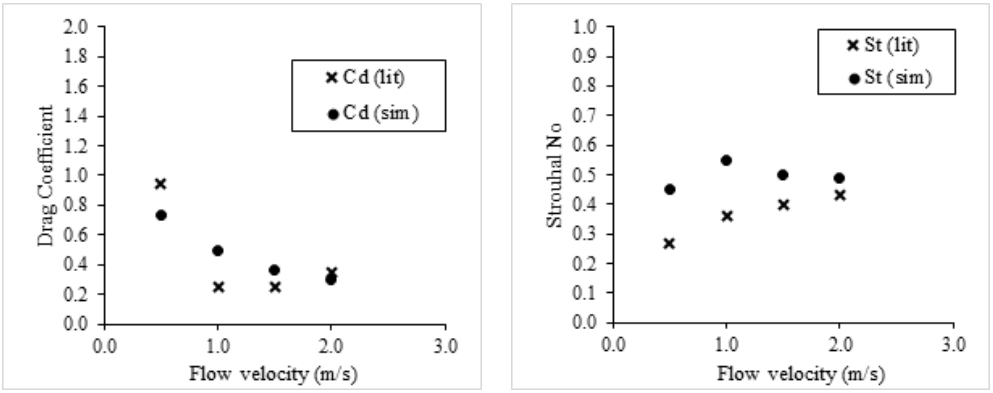

(a) (b)

Fig. 7. Validation of simulation model (a) Drag coefficient (b) Strouhal number

3.2. Drag Coefficient and Strouhal Number Analysis

Strouhal, St number is one of the fluid characteristic that has been used as indicator for the formation of shedding vortex. The higher St number will produce the more shed vortices around body and more aggressive. In this analysis, the effect of fairing geometry on the formation of vertex shedding is conducted in order to supress the number of vortices around riser. Figure 8 shows the comparative analysis between the flow pattern of bare cylinder and cylinder with fairing geometry at the flow speed of 1.0 m/s. The figure illustrated that the vortex shedding formation is relatively aggressive, faster and very close to the main structure for bare cylinder, while for cylinder with fairing, the vortex shedding formation is less aggressive, slower and further away from the main structure.

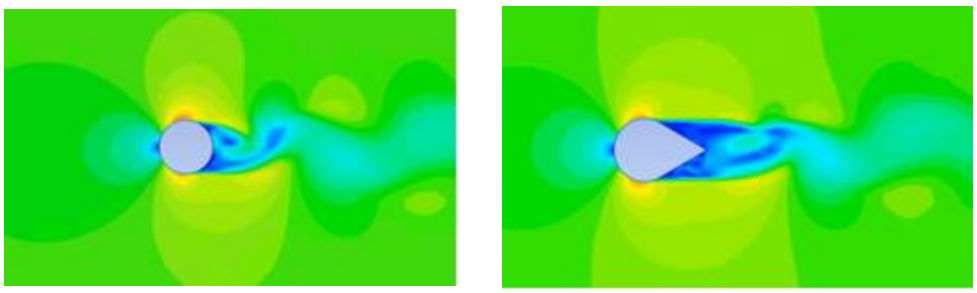

(a) (b)

Fig. 8. Comparison of flow contour for (a) bare cylinder and (b) cylinder with fairing subjected to flow speed of 1.0 m/s

Figure 9(a) has proven that cylinder bar with fairing geometry will provide drag coefficient ≤ 0.3. And surprisingly, the increases of fairing chord length can reduce the drag coefficient. The figure shows fairing of 1.5D obtained the lowest drag coefficient for all flow speed. Besides that, Figure 9(b) also observed the fairing of 1.5D shows the lower St number compare to fairing of 1.25D. Means that, vortex shedding formation in the 1.5D fairing is less aggressive and far from body compare to 1.25D fairing.

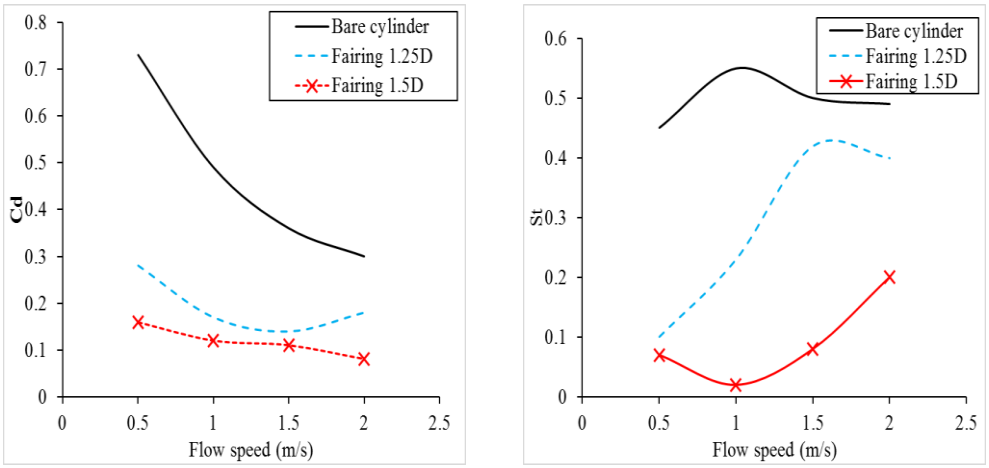

Fig. 9. Flow characteristic (a) Drag coefficient, Cd and (b) Strouhal number, St.

3.3. Drag Coefficient and Lift Coefficient Analysis

Lift coefficient is other characteristic that need to be considered in VIV suppression device design. Too high lift coefficient in body device will moves a riser aggressively. From Figure 10(a), at the flow speed of 0.5 m/s, drag coefficient decreases from bare cylinder to fairing with increasing chord length. Lift coefficient also decreases from bare cylinder to fairing with increasing chord length. Lift coefficient is more dominant than drag coefficient for all cylinder type. It would be possible that the cylinder with fairing length of 1.5D is optimum geometry parameter for the flow speed of 0.5 m/s in the studied configurations.

Figure 10(b), 10(c) and 10(d) also shows that at the flow speeds of 1.0 m/s 1.5 m/s and 2.0 m/s, drag coefficient decreases from bare cylinder to fairing with increasing chord length. Lift coefficient also decreases from bare cylinder to fairing with 1.25D chord length, but increases back on fairing with 1.5D chord length. Lift coefficient is more dominant than drag coefficient for all cylinder type. It would be possible that the cylinder with fairing length of 1.25D is optimum geometry parameter for the flow speeds of 1.0 m/s 1.5 m/s and 2.0 m/s in the studied configurations.

It is found from this investigation that increasing the fairing chord length will reduce the drag coefficient (CD) of the cylindrical structure, but not necessarily to reduce the lift coefficient further as the drag coefficient (CD) getting greater. The lift coefficient (CL) could be lowest at the optimum fairing chord length. Besides that, St number is decreases as the cord length of fairing increases. Validation on numerical solution model shows that results for few parameters such as drag coefficient (CD), and Strouhal number (St) are in good agreement with the data from the literature. Thus, reliability of the CFD solution method executed in this study is relatively solid. Hence, this investigation is referable for future studies.

When a cylindrical structure such as riser and conductor in oil and gas industry are subjected to continuous current flow, additional accessories such as faring can be fabricated on the structure to increase service life by reducing the drag as well as lift force, and thus reducing a damage to the structure. This will be a great beneficial to the platform operator in terms of reducing the maintenance cost.

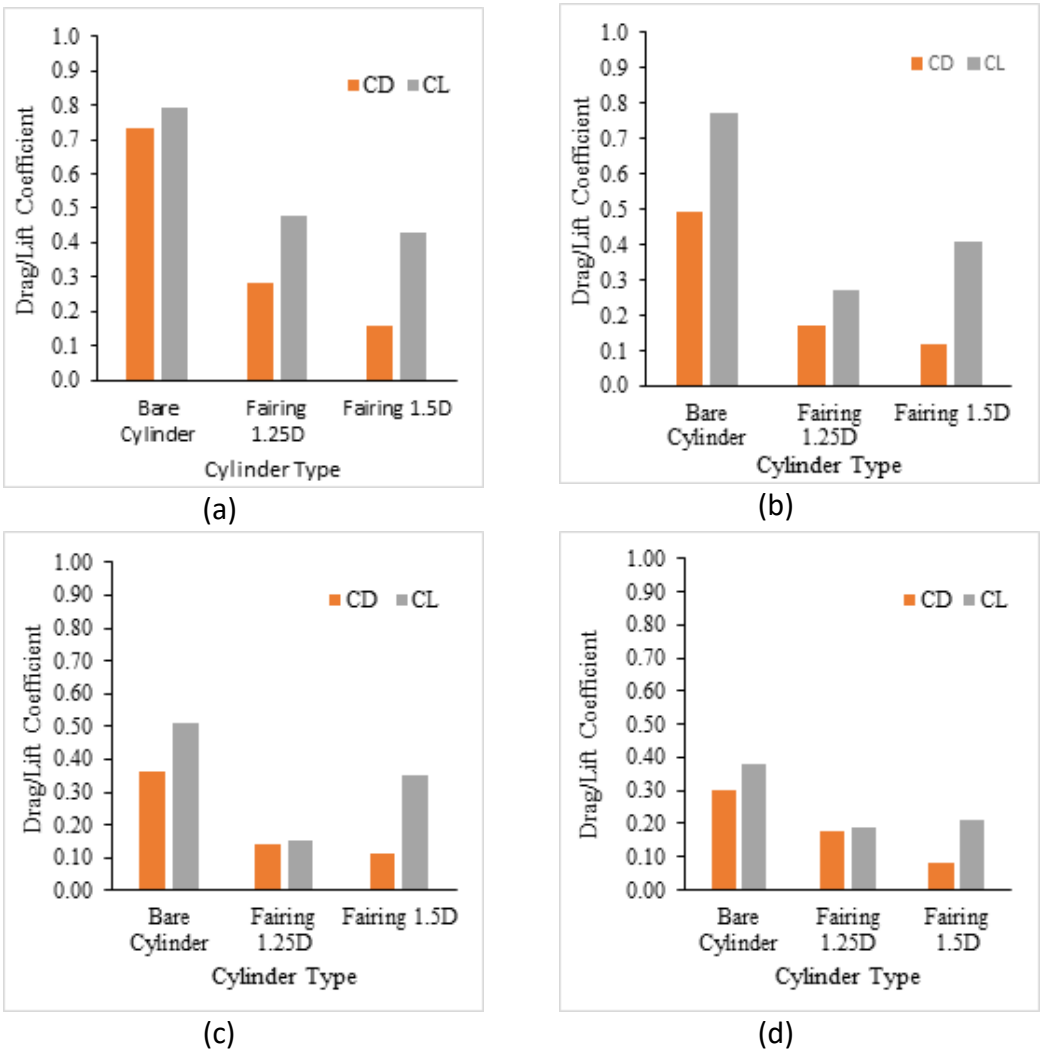

Fig. 10. Trend of drag and lift coefficient for different cylinder conditions at different flow speeds (a) 0.5 m/s (b) 1.0 m/s (c) 1.5 m/s (d) 2.0 m/s)

4. Conclusions

In order to analyse the effectiveness of fairing geometry as a method to supress VIV, comparative analysis on drag coefficient and lift coefficient between cylinder riser with and without fairing shape have been conducted numerically. Besides that, the effect of fairing chord length on drag coefficient and lift coefficient have been analysed so as the optimum geometry parameter can be determined. All the analysis can be concluded as bellows:

- Cylinder riser with fairing geometry has reduced the vortex shedding formation near to main structure.
- Vortex shedding formed by cylinder riser with fairing geometry is less aggressive and slower than cylinder riser without fairing geometry.
- At flow velocity, v = 0.5m/s, fairing geometry with chord length of 1.5D shows the lowest value of drag coefficient and lift coefficient.
- At flow velocity 1.0m/s≤v≤2.0m/s, fairing geometry with chord length of 1.25D shows the lowest value of lift coefficient and CL-CD ratio.

Acknowledgement
Authors are grateful to the supervision and guidance from the academicians in UTM during the research period.

References
[1] Chakrabarti, Subrata K., and Ralph E. Frampton. "Review of riser analysis techniques." *Applied ocean research* 4, no. 2 (1982): 73-90.
[2] He, Wei, Shuzhi Sam Ge, Bernard Voon Ee How, and Yoo Sang Choo. Dynamics and control of mechanical systems in offshore engineering. London: Springer, 2014.
[3] Blevins, Robert D. "Flow-induced vibration." (1990).
[4] Nakamura, Tomomichi, Shigehiko Kaneko, Fumio Inada, Minoru Kato, Kunihiko Ishihara, Takashi Nishihara, Njuki W. Mureithi, and Mikael A. Langthjem, eds. Flow-induced vibrations: classifications and lessons from practical experiences. Butterworth-Heinemann, 2013.
[5] Gao, Yun, Shixiao Fu, Leixin Ma, and Yifan Chen. "Experimental investigation of the response performance of VIV on a flexible riser with helical strakes." *Ships and Offshore Structures* 11, no. 2 (2016): 113-128.
[6] Siti Hajar Adni Mustaffa, Fatimah Al Zahrah Mohd Saat, Ernie Mattokit, "Turbulent Vortex Shedding across Internal Structure in Thermoacoustic Oscillatory Flow," *Journal of Advanced Research in Fluid Mechanics and Thermal Sciences*, vol. 46, no. 1, p. 10, 2018
[7] Choi, Haecheon, Woo-Pyung Jeon, and Jinsung Kim. "Control of flow over a bluff body." *Annu. Rev. Fluid Mech*. 40 (2008): 113-139.
[8] Lou, Min, Zhiwei Chen, and Peng Chen. "Experimental investigation of the suppression of vortex induced vibration of two interfering risers with splitter plates." *Journal of Natural Gas Science and Engineering* 35 (2016): 736-752.
[9] Holland, Vegard, Tahsin Tezdogan, and Elif Oguz. "Full-scale CFD investigations of helical strakes as a means of reducing the vortex induced forces on a semi-submersible." *Ocean Engineering* 137 (2017): 338-351.
[10] Borges, F. C. L., N. Roitman, C. Magluta, D. A. Castello, and R. Franciss. "A concept to reduce vibrations in steel catenary risers by the use of viscoelastic materials." *Ocean Engineering* 77 (2014): 1-11.
[11] Nishi, Yoshiki, and Phan Viet Doan. "Distribution of damping device on riser pipe in sheared currents." *Ocean Engineering* 104 (2015): 489-499.
[12] Gao, Yun, Jiadong Yang, Youming Xiong, Menghao Wang, and Da Lu. "VIV response of a long flexible riser fitted with different helical strake coverages in uniform and linearly sheared currents." *Ships and Offshore Structures* 12, no. 4 (2017): 575-590.
[13] Zhang, Wen-Shou, and Dong-Dong Li. "Active control of axial dynamic response of deepwater risers with Linear Quadratic Gaussian controllers." *Ocean Engineering* 109 (2015): 320-329.
[14] He, Wei, Xiuyu He, and Shuzhi Sam Ge. "Modeling and vibration control of a coupled vessel-mooring-riser system." *IEEE/ASME Transactions on Mechatronics* 20, no. 6 (2015): 2832-2840.
[15] He, Wei, Xiuyu He, and Shuzhi Sam Ge. "Vibration control of flexible marine riser systems with input saturation." *IEEE/ASME Transactions on Mechatronics* 21, no. 1 (2016): 254-265.
[16] Azmi, Azlin Mohd, and Tongming Zhou. "Effect of Screen Geometry on the Vortex Formation behind a Circular Cylinder." *Journal of Advanced Research in Fluid Mechanics and Thermal Sciences* 44, no. 1 (2018): 47-54.
[17] Meng, Dan, and Chongji Zhu. "Synergetic analysis and possible control of vortex-induced vibrations in a fluid-conveying steel catenary riser." *Journal of Ocean University of China* 14, no. 2 (2015): 245-254.
[18] Rahman, Md Mahbubar, Md Mashud Karim, and Md Abdul Alim. "Numerical investigation of unsteady flow past a circular cylinder using 2-D finite volume method." *Journal of Naval Architecture and Marine Engineering* 4, no. 1 (2007): 27-42.
[19] Patnana, Vijaya K., Ram P. Bharti, and Raj P. Chhabra. "Two-dimensional unsteady flow of power-law fluids over a cylinder." *Chemical Engineering Science* 64, no. 12 (2009): 2978-2999.
[20] Mittal, S., and V. Kumar. "Vortex induced vibrations of a pair of cylinders at Reynolds number 1000." *International Journal of computational fluid dynamics* 18, no. 7 (2004): 601-614.
[21] Shao, J., and C. Zhang. "Large eddy simulations of the flow past two side-by-side circular cylinders." *International Journal of Computational Fluid Dynamics* 22, no. 6 (2008): 393-404.
[22] Bourguet, Rémi, George E. Karniadakis, and Michael S. Triantafyllou. "Lock-in of the vortex-induced vibrations of a long tensioned beam in shear flow." *Journal of Fluids and Structures* 27, no. 5-6 (2011): 838-847.
[23] Patil, Pratish P., and Shaligram Tiwari. "Numerical investigation of laminar unsteady wakes behind two inline square cylinders confined in a channel." *Engineering Applications of Computational Fluid Mechanics* 3, no. 3 (2009): 369-385.

[24] Mhalungekar, Chandrakant D., and Swapnil P. Wadkar. "CFD and Experimental analysis of vortex shedding behind D-shaped cylinder." *International Journal of Innovative Research in advanced engineering* (IJIRAE) (2014).
[25] Kianifar, Ali, and Edris Yousefi Rad. "Numerical simulation of unsteady flow with vortex shedding around circular cylinder." *momentum* 2 (2010): 1.
[26] Roshko, Anatol. "Experiments on the flow past a circular cylinder at very high Reynolds number." *Journal of Fluid Mechanics* 10, no. 3 (1961): 345-356.
[27] Lienhard, John H. Synopsis of lift, drag, and vortex frequency data for rigid circular cylinders. Vol. 300. Technical Extension Service, Washington State University, 1966.
[28] Hong, Keum-Shik, and Umer Hameed Shah. "Vortex-induced vibrations and control of marine risers: A review." *Ocean Engineering* 152 (2018): 300-315.
[29] Asyikin, Muhammad Tedy. "CFD simulation of vortex induced vibration of a cylindrical structure." Master's thesis, Institutt for bygg, anlegg og transport, 2012.